RSC Advances

ROYAL SOCIETY OF CHEMISTRY

www.rsc.org/advances

Novel surfactant aided micellar system of oxidation inhibitors in clotrimazole bioadhesive gel: Development, characterization, *in vitro* and *in vivo* antifungal evaluation against *Candida* clinical isolates

Varun Bhardwaj [a], Jitender Monga [b], Amit Sharma [c], Shailesh Sharma [d], Arun Sharma [a], Poonam Sharma [a, *]

[a]*Department of Biotechnology, Bioinformatics and Pharmacy, Jaypee University of Information Technology, Waknaghat, Solan, Himachal Pradesh 173234, India.*
[b]*Department of Medical Urology, Postgraduate Institute of Medical Education and Research (PGIMER), Chandigarh, 160012, India.*
[c]*Department of Medical Parasitology, Postgraduate Institute of Medical Education and Research (PGIMER), Chandigarh, 160012, India.*
[d]*Department of Pharmaceutics, ASBASJSM College of Pharmacy, Bela, Ropar, Punjab 140111, India.*

Corresponding Author (*):

Dr. Poonam Sharma, Tel: +91–1792–239389, Fax: +91–1792–245362

Email: drpoonamsharma@rediffmail.com, varunmilton@yahoo.com

Abstract

Clotrimazole (CLZ) is a widely used antifungal agent with poor aqueous solubility, which requires the development of new drug delivery systems in order to improve its therapeutic activity. However, butylatedhydroxy anisole (BHA) and butylatedhydroxy toluene (BHT) has been known as potential antioxidants with antimicrobial property. In an attempt to develop better formulation with antifungal profile, surfactant aided antioxidants micellar system was dispersed within clotrimazole gel formulation. Initially, the gel library was prepared and subjected to *in vitro* evaluation. Based on *in vitro* release and kinetic profile, best three formulations were selected for further analysis. Moreover, *in vitro* antifungal activity (MIC) and fractional inhibitory concentration index (FICI) against different drug resistant and susceptible *Candida* isolates were carried and directed to the best among 27 formulations. The optimized best selected formulation was thereafter evaluated via morphology studies and *in vivo* antifungal evaluation. Morphology studies depicted the distribution of micellar structures within the polymeric gel network as well as the contact activity mechanism against *Candida albicans*. The physicochemical characterization showed that average micellar size was lower than ~ 160 nm, low polydispersity index, negative zeta potential and gel pH 6.9. After 60 days, no significant change was observed within the formulation. Photostability studies revealed that antioxidants' eminently inhibits the drug degradation under UV radiations with improved drug stability. In addition, *in vivo* antifungal activity was carried out on experimentally induced cutaneous infection in immunosuppressed *Sprague Dawley* (SD) rats. The *in vivo* study confirmed the maximum therapeutic efficacy, as the lowest number of cfu/ml was recorded. Conclusively, this study provide a good skin targeting effect and may be promising for stable and effective topical delivery of CLZ offering maintained localized effect.

Key words: Antioxidant; Micellar system; Clotrimazole; Topical gel; Antifungal activity

1. Introduction

Fungal infections are caused by microscopic organisms that can invade the epithelial tissue. The fungi kingdom includes yeasts, molds, rusts and mushrooms which are commonly found on the skin, mouth, throat, stomach, colon, rectum and vagina [1, 2]. Whenever proliferation of this kind of organism occurs, it can produce symptomatic infections of the skin, mouth, vagina or intestine [3]. The incidence of mycoses especially superficial fungal infections is increasing and more than 25% of the world's population is affected [4]. It is found that disease progression is more rapid and severity increases in patients with compromised immune function. *Candida* species are one of the most important fungal pathogens which are responsible for variant life–threatening disorders [5]. Among antimycotics, clotrimazole (CLZ) is a broad spectrum antifungal antibiotic belonging to class of 'Azoles' used as first line treatment for various fungal infections [6]. According to WHO, it is an effective antifungal agent in topical infections, and also listed in 'Essential Drugs list' [7]. One percent solution or cream of CLZ is reported to be clinically effective for topical treatment especially against *Candida* species [7]. Besides this, CLZ is a poorly water–soluble drug, which affects its local absorption thus having low bioavailability [8]. In this context as reported in literature [9, 10], bioadhesive formulations such as tablets, nanostructured carriers, gels and microemulsion were developed in order to increase the residence time of the dosage form and/or to enhance local bioavailability.

Antioxidants are bioactive moieties that originally can be referred to molecules that retard or prevent the utilization of oxygen by human tissues and known to prevent the oxidative system as a whole. In recent years, they have been commonly employed in combination with many drugs and bioactive compounds [11, 12]. They are also been reported to influence antimicrobial or antifungal activity in case of concomitant administration with

standard drugs. Butylated hydroxyanisole (BHA) and butylated hydroxytoluene (BHT) containing alkyl groups has been classified as hindered phenols and are considered to be effective when used in various cosmeceutical or pharmaceutical formulations. BHA and BHT are also known to possess antimicrobial activity against various pathogenic and non–pathogenic organisms [13]. Besides the favorable use of these antioxidants recently they have been reported for the toxic effects and poor bioavailability [14]. Thus, the use of these phenolic antioxidants is to regulate the permitted percentage of the compound as well as their concentration limits. However, surfactants which have been extensively studied for its micellization properties and employed as effective vehicle for the solubilization, binding or entrapment medium to overcome such problems likely, toxicity, low bioavailability and bioactivity. Surfactants and polymeric systems play an eminent role in modern drug delivery, where they may be used to control drug release rate, enhance effective molecule solubility, reduce toxicity or facilitate control of active molecule uptake. In fact even earlier, micellar solutions have been proposed as effective strategies for bioactive compound delivery [15, 16].

With regard to our previous reported physicochemical studies [17-22] on micellar behavior of three different surfactants as; anionic – sodium dodecyl sulfate (SDS), cationic – cetyltrimethylammonium bromide (CTAB) and nonionic – *tert*–octylphenol ethoxylated or Triton X – 100 (TX100) in presence of BHA and BHT, the study was extended to dispersion of surfactant immobilized BHA/BHT micellar solutions into carbopol 940 based CLZ topical gel. Polymer carbopol 940 was employed because of its advantageous bio–adhesive property and suits best in case of hydroalcoholic formulations [23, 24]. The chemical structures of studied active pharmaceutical molecules have been presented in Fig. 1. In particular, the present study was conducted to develop and characterize micellar immobilized BHA, BHT or BHA + BHT with CLZ in a bio–adhesive three dimensional gel structure in order to increase drug

residence time and stability, and then optimization of the best formulation among the formulated gel library with three different surfactant systems (on the basis of *in vitro* profile). Afterward, further evaluation in terms of (i) *in vitro* antifungal activity on 30 different *Candida* clinical isolates, (ii) morphology study via electron microscopy tools (SEM and TEM), (iii) skin irritation study in addition to histological toxicity profile of the best formulation, (iv) visualization of transport of formulation using confocal laser scanning microscopy and, (v) *in vivo* antifungal activity (mouse model).

2. Materials and methods

2.1. Materials

Clotrimazole (99.1%) was obtained from Glenmark Pharmaceutical Limited, (Himachal Pradesh) India. Butylated hydroxyanisole (BHA), butylated hydroxytoluene (BHT), sodium dodecyl sulfate (SDS), cetyltrimethylammonium bromide (CTAB), *tert*–octylphenol ethoxylate or Triton X – 100 (TX100) (AR grade and purity > 99%) and ethanol (EtOH) absolute (purity ≥ 99.9%), were obtained from Merck Chemicals. Freshly prepared double distilled water obtained by double distillation unit obtained from HARCO & Co. was used in the study.

In present study, male *Sprague Dawley* (SD) rats (160-180 g) were used. Animals were housed in plastic cages in a 12 h dark-light cycle, with controlled temperature (25 °C) and humidity (70%). Water and food were provided *ad libitum* throughout the study. The animals were housed in Central Animal Facility (CAF) of ASBASJSM college of Pharmacy, Bela, Ropar, India. All protocols were approved by Institutional Animal Ethics Committee (IAEC), and experiments were performed in accordance with CPCSEA.

2.2. Analytical procedure

The experiments were performed on Nanodrop Spectrophotometer (Thermo Scientific). Clotrimazole was detected at 261 nm in optimized ratio of phosphate buffer (7.4): methanol. The method was validated according to the ICH guidelines to determine drug within the developed gel system. The method was found to be linear (r^2 = 0.998), and robust (relative standard deviation was < 4% for all parameters) in the concentration range of 10–500 µg/ml obeying the Lambert Beer range [25].

2.3. Preparation of micellar solution with SDS, CTAB and TX100

From our previous thermo–physical analysis studies [17-22], the critical micelle concentration (CMC) with most feasible and thermodynamic stable concentration was taken into consideration. Among the studied concentrations, 30% v/v EtOH was found to be the most feasible and thermodynamically controlled system which was lately utilized in the present formulation studies. It was found and reported that the presence of additives facilitated the micellization process, resulting early micelle formation. In this context, three optimized surfactant's (SDS, CTAB and TX100) concentrations near/ above CMCs were selected, respectively. Likely, for SDS (6.0, 7.0 and 8.0 mmol kg^{-1}), CTAB (0.8, 0.9 and 1.0 mmol kg^{-1}) and TX100 (0.20, 0.22 and 0.24 mmol kg^{-1}) were the selected concentrations. Optimized concentrations were utilized for BHA and BHT with respect to obtained CMC values of surfactant in 30% v/v EtOH. All the calculate concentrations based on thermo–physical analysis are presented in Table 1. Accordingly, BHA (5 mg) and BHT (4 mg) were added to surfactant hydroethanolic solutions (30% v/v EtOH) andthe mixture was stirred at room temperature at 700 rpm for 24 h. Afterward the mixture was centrifuged at 10000 rpm at 25 °C for 15 min and then upper solution was filtered through a nylon syringe filter (pore size 0.2 µm, Whatman Inc., USA). The prepared micellar solution was dispersed into the gel.

2.4. Preparation of Gel Library

The gel base was prepared by dispersing the polymer (carbopol 940) in distilled water. Carbopol 940 was chosen due to its hydrophilic nature and bioadhesive property, which might result in an increased residence time of the compounds at the site of absorption when gets interacted with the topical membrane. The polymer was weighed accordingly for each formulation and then soaked in distilled water for 2 h prior to use. Afterward, it was dispersed in distilled water under magnetic stirring for 1 h so as to obtain a homogenous gel base of 1% w/w. Thereafter, SDS/CTAB/TX100 immobilized BHA, BHT and BHA + BHT were added to the gel base. Triethanolamine (TEA), pH = 7.0 was added drop–wise to obtain neutralized carbopol gels and were further subjected to constant stirring.

2.5. Characterization

2.5.1. pH, viscosity and spreadability

The pH of prepared gel library of 27 formulations was verified by directly immersing the electrode of a calibrated Cyber scan 2500 pH meter in the formulations. All the measurements were carried out at room temperature (25 ± 2 °C) in triplicate of batch. The viscosity measurements of the prepared gels were carried out using Brookfield viscometer (R/S–CPS Rheometer – Brookfield Engineering Laboratories, UK). Spreadability was calculated by using the formula; $S = M \times L / T$, where, M was the weight tied to upper slide, L was the length of glass slides, and T was the time taken to separate the slides.

2.5.2. In vitro drug release study

The diffusion studies of the prepared gels were carried out using Franz diffusion cell having the diameter of 0.50 cm^2. For studying the dissolution release profile of formulated gels, a cellullose membrane (pores size 0.22µm) was used which was hydrated in phosphate buffer

pH 7.4 prior to use for 24 h before placing them between donor and receptor compartments. The receptor compartment contained 18 ml phosphate buffer at pH 7.4, under magnetic stirring. The temperature of the Franz diffusion cells was maintained at 37 ± 0.5 °C. Gel sample (0.5 g) was taken in cellophane membrane and the diffusion studies were carried out at 37 ± 1 °C. Samples were withdrawn periodically at 0.5, 1, 2, 3, 4, 5, and 6 h and each sample was replaced with equal volume of fresh dissolution medium to maintain the sink conditions. Then the samples were analyzed spectrophometrically by using phosphate buffer pH 7.4 as reference.

2.5.3. Mathematical modeling of release profiles

The release kinetics allows the measurement of some important physical parameters, such as the drug diffusion coefficient and resorting to model fitting on experimental release data. The data from the *in vitro* study was fitted to the following kinetic models to determine the kinetics of drug release. The suitability of equation in judged on the basis of best fit to the equation using statistical indicators likely, R^2. The release profiles of all the formulations were analyzed by model–dependent approaches; the Zero order, the first order model, the Higuchi model and the Korsmeyer–Peppas model, using specific equations as shown in **Table 2**, [26, 27].

2.6. In vitro antifungal activity against Candida isolates

2.6.1. Fungal strains

Fungal strains; *Candida* clinical isolates, used in the present study were collected from Department of Medical Microbiology, Postgraduate Institute of Medical Education and Research, Chandigarh, India and Indra Gandhi Medical College, Shimla, Himachal Pradesh, India. Among obtained 30 clinical isolates, 11 were fluconazole (FLZ) resistant *C. albicans,*

4 miconazole (MLZ) resistant *C. albicans,* 3 FLZ susceptible *C. albicans,* 8 FLZ susceptible *C. tropicalis,* and 4 FLZ susceptible *C. glabrata* clinical isolates.

2.6.2. In vitro antifungal activity

Standardized protocol M27–A2, CLSI (Clinical and Laboratory Standards Institute) was followed to perform the experiment [28]. The inocula were performed after growth (48 h/ 35 °C) on Sabouraud dextrose agar. The colonies were suspended in 0.85% sterile saline and this suspension was homogenized in a vortex mixer for 15 s; after that, cell density was set in a spectrophotometer and transmittance (λ = 630 nm) was adjusted to match standard 0.5 on the McFarland scale (1×10^6 to 5×10^6 cells/ ml). In the sequence, a 1:50 dilution in water was done, followed by a 1:20 dilution in RPMI 1640 medium, resulting in a final concentration of $1.5 \pm 1.0 \times 10^3$ cells/ml [29]. The micro–dilution technique [30] was performed in polystyrene sterile plates with flat–bottom, disposable, with 96 wells diluted in RPMI 1640 buffered broth. To each well micro–dilution plate were added 100 µl of the standardized inoculum. The plates were incubated at 35 °C for 48 hrs and then 10 ml of 0.5% 2,3,5–triphenyltetrazolium chloride dye was added to all wells, and the plates were re–incubated at 35 °C for 20 min. Afterward, the minimum inhibitory concentration (MIC) was determined.

Among several *in vitro* methodologies developed to assess *in vitro* pharmacodynamic interactions, checkerboard techniques are usually employed to study antifungal combinations. The interaction of drug combinations (BHA+BHT and CLZ) was analyzed using the Fractional Inhibitory Concentration Index (FICI), which is based on the Loewe additivity zero–interaction theory. FICI represents the sum of FICs of each compound tested, where the FIC is determined by; each compound/drug by dividing the MIC of each drug when used in combination by the MIC of each drug when used alone. The drug interactions were classified

as synergic (FICI ≤ 0.5), additive (FICI 0.5 – 1.0), showing no interaction between FICI = >0.5 – 4, and antagonistic (FICI > 4) [31].

2.7. Morphological study

The surface morphology was characterized by scanning electron microscope (S–3400N, Hitachi, Japan). The gel sample was deposited on a glass cover slip previously adhered to a metallic stub by a bio–adhesive carbon tape. Afterward, the sample was air–dried before analysis and coated with gold to obtain a conducting surface. Finally, the sample was analyzed by scanning electron microscopy (SEM) in vacuum. The SEM was obtained for the same formulation at different interval of time, likely, after preparation, after ~ 1 month and ~ 9 months. Transmission electron microscope (Hitachi H-7500 80 kV; Ibaraki, Japan) was used to visualize the dispersed micellar structures within the gel.

The visualization of morphology of *C. albicans* was carried out by TEM [32, 33]. Initially untreated *C. albicans* was visualized and afterward, it was treated with the optimized best formulation at a concentration of 10 μg/ml. The images were taken at different interval of time likely; 15 min, 2 h and 6 h in order to gain information on the action of formulation on infection site.

2.8. Physical and photo–stability studies

The formulation was stored for 3 months after preparation in order to evaluate changes in drug content, pH, viscosity, and spreadability. Photo–stability study for CLZ was performed to quantify the drug after exposure to UVC light for 14 h. Quartz cuvettes were filled with CLZ methanolic solution (C–1) and CAT–3S (CLZ with dispersed BHA + BHT micelles) and exposed to UV radiation (TUV lamp – 30 W) in a chamber at a fixed distance from each other for 14 h. In order to compare, the CLZ methanolic solution was covered with aluminium paper as dark control. The protection of CLZ against the UVC radiations was evaluated by quantifying the remaining drug using HPLC.

2.9. Skin Irritation study and toxicity profiling

Healthy male *Sprague Dawley* (SD) rats with average weight of 160–180 g were selected. Initially, hairs were removed from the dorsal side of rats (2 cm × 3 cm) with the help of electric clipper without damaging the skin. The control group was treated with normal saline and gel was applied to the treatment group three times a day for three days consecutively (n = 5). The visual observations were carried out at regular intervals of 12, 24, 48, and 72 h for various symptoms such as erythema, flakiness, dryness, erythema or edema. The irritation scores of the test area were obtained by judging the extent of erythema and edema according to the literature [34]. Erythema and edema were graded as follows: 0 for no visible reaction, 1 for just present reaction (barely perceptible-light pink), 2 for slight reaction (light red), 3 for moderate reaction (moderate red), and 4 for severe reaction (extreme redness).

In vivo toxicity test was conducted to gain better perception. Twelve animals were randomly divided into two groups. The first group (untreated) served as control, whilst second group received the treatment (CAT-3S). The treatments were given via topical application. After 24 h of treatment, the remnants of the gels were gently washed away from the skin surface using adsorbent cotton dipped in physiological saline. Again the dorsal sites of treated animals were inspected for any erythema or edema. Thereafter, animals were sacrificed. Major organs likely, skin, liver, kidney, and intestine were taken out. The excised skin sample and isolated organs were presented in 10% formalin for histopathological examination. Sections were fixed and blocks were made following the procedure as reported[35]. The sections were stained with eosin-hematoxylin (H and E) to determine gross histopathology.

2.10. Confocal laser scanning microscopy (CLSM)

The depth and mechanism of the skin permeation of Rhodamine B within prepared gel system was investigated in absence of drug using CLSM [36]. The formulation was applied to

the dorsal skin of rats for 8 h. The rat was then sacrificed by heart puncture and dorsal area was excised and cleaned with a thin stream of water to remove any residual gel. Afterward, the skin was placed on aluminium foil and adhering fat was removed. The excised skin was sliced and examined with CLSM (FV fluoview 1000; Olympus, Tokyo, Japan).

2.11. In vivo antifungal study

2.11.1. Preparation of Inoculum

Clinical isolate of *Candida albicans* (PGI/DLM54) was used to infect the animals. Cultures were revived from glycerol stock onto sabouraud dextrose agar (SDA) slants for 48 h at 35 °C before use. Cells were suspended by vortexing a single pure colony in pyrogen free normal saline and subsequently diluted to a final concentration of 2×10^6 cells/ml. The colonies were pure as identified from the morphology, and none of the cell suspensions were contaminated with any other organism.

2.11.2. Cutaneous infection

Each animal's back was shaved with an electric clipper and an approximately 3.0 cm^2 area was marked on each animal's back. The marked area was infected with 10^7 cfu/ml suspensions by gently rubbing onto the skin for 3 days with the help of a sterile, cotton–tipped swab until no more visible fluid was observed [37]. Infection was produced under an occlusive dressing and the infected area was covered with a sterile adhesive bandage, held in place with extra–adherent tape for 48 h before treatment began [38]. Control animals were infected in the same manner; however, they did not receive any formulation treatment.

2.11.3. In vivo efficacy

In vivo antifungal activity for the most potent formulation was carried out by using male SD rats (160–180 g). All animals were rendered immunosuppressed by injecting cyclophosphamide (150 mg/kg) intraperitoneally 4 days and 1 day before experimental infection. Treatment began 24 h after the infection was induced and test formulation was

topically applied once daily for 3 consecutive days. The experimental animals were divided into four groups each containing 6 animals and the test animals were treated topically. Group 1 was treated with plain drug (1 mg/cm^2), group 2 with formulation CAT–3S at dose level of 1 mg/cm^2; group 3 with formulation CAT–3S at dose level of 5 mg/cm^2; and group 4 served as the control. All animals were sacrificed 48 h following the last treatment and 3.0 cm^2 of skin from the infected sites was excised. The infected skin samples were collected, washed and then plated into SDA culture media and incubated for 48 h at 37 ± 1 ºC, and then viable CFUs were counted [39].

2.12. Statistics

The antifungal efficacy against *C. albicans* was analyzed with two–way ANOVA and followed by a Bonferroni test using graph pad prism software.

3. Result and discussion

3.1. Physicochemical characterization

3.1.1. Preliminary characterization of gel formulation library

After preparation, the total number of formulations was subjected to preliminary physicochemical examination. The data has been provided in Table 3. All the gels were found with white opaque to translucent appearance. No visible precipitation was observed in all the formulations, whilst smooth and homogeneous texture was obtained. Given that pH of skin can vary according to age which might affects the drug permeation rate, the pH was found close to neutral value i.e. 7.0 attributing to better bioadhesive property. Considering pH determination of all 27 formulations, the values were found to lie within a range of 6.8 ± 0.2 – 7.3 ± 0.1. The viscosity values of all the gels were found in the range of 47719 ± 19 to 47849 ± 35 centipoise (cP). Interestingly, the increase of rotation speed did not significantly change the viscosity of the gels, revealing the formation of stable gel structure. This might be

because of carbopol 940 that forms a physically bonded network in which movement of the dispersion medium is restricted by intercalating three dimensional network of solvated particles. Also, carbopol consists of twisted strands often tied together by stronger types of Vander Waals Forces to form stable network throughout the system. From a patient compliance perspective, spreadability is a pivot for topical gel formulation. The formulations were found to exhibit good spreadability by weight (in a range of 11.00 ± 0.32 – 15.53 ± 0.12 g.cm/s).

Chemical interaction for CLZ and carbopol 940 was carried out via FTIR analysis. Initially the substantial peaks were characterized and analyzed for individual compound, in addition to that, FTIR was obtained for the admixture of CLZ and carbopol 940 as presented in Fig. 2. The Fig. 2(a) represent the FTIR of carbopol 940 and the peaks at 3037.89 cm^{-1} and 2930.88 cm^{-1} represent OH stretching vibration. The prominent band at 1707.59 cm^{-1} correspond to carbonyl C=O stretching vibration whereas the band at 1242.70 cm^{-1} represent C-O-C of acrylates. The band at 803.79 cm^{-1} represents the plane bending of CH. On the other side, the FTIR spectrum of CLZ was characterized by the bands at 3007.70 cm^{-1} (aromatic CH stretching); 1495.70, 1438.00 cm^{-1} (benzene ring stretching); 907.73, 829.00, 769.30, 747.37 cm^{-1} (CH stretching); 1210.03 cm^{-1} (CN stretching); and 1080.50 cm^{-1} (chlorobenzene), respectively [Fig. 2(b)]. Comparative FTIR revealed the absence of any kind of chemical interaction or incompatibility, attributing that CLZ and carbopol 940 are compatible within the system. All of the characteristic bands remained unaffected in the obtained spectrum of CLZ + carbopol 940 admixture sample [Fig. 2(c)].

3.1.2. In vitro drug release and mathematic modeling

The ability of gel formulations to deliver CLZ was examined by determining the drug release rate. *In vitro* release study was conducted in optimized ratio of phosphate buffer (pH 7.4) and

methanol (6:4). Fig. 3. shows the cumulative percent release of reduced best three formulations containing antioxidants' micellar system with different surfactant i.e. SDS, CTAB and TX100. For all the formulations, the release data has been presented in Table 4 and release kinetics as supplementary data (S1). To gain better comparison, the study was initially optimized and conducted for 6 h. In comparison to plain drug, CAT-3S and CAT-3X showed higher release with initial slight burst then controlled, which might be because of the present additives providing additional driving force and afterward controlled by polymeric network structure of gel. It is important to note down that higher localized release is required in treatment of superficial localized infections. In order to describe the drug release profiles from the gel, the *in vitro* release data were fitted into mathematic models and analyzed. The *in vitro* release data were fitted into Zero order, First order, Higuchi and Korsmeyer-Peppas kinetic equations. It was found that all the formulations had a good fit to the zero order equation, likely, R^2 = 0.956 for CAT-3S, R^2 = 0.997 for CAT-3C, and R^2 = 0.9995 for CAT-3X, respectively. Interestingly, CAT-3S was found to have maximum R^2 in case of Higuchi as well as Korsmeyer-peppas model. Korsmeyer-peppas model suggested that the release followed diffusion controlled mechanism (n = 0.3). Results showed release exponent n values of about 0.3 attributing that drug release is driven by diffusion transport, following Fick's law of diffusion, in other words, drug release is concentration dependent. The kind of release obtained is known to reduce the induction of fungi tolerance to the antifungal drug.

3.2. In vitro antifungal activity

The *in vitro* antifungal activity of optimized best three formulations viz., CAT-3S, CAT-3C and CAT-3X was assessed. The MIC (μg/ml) values were obtained and presented in Table 5-7. Lower the MIC values are indicative of higher antifungal activity. The antifungal study was conducted against clinically collected samples. Most of the obtained clinical isolates

were FLZ resistant *C. albicans* as shown in Table 5-7. For this reason MIC for FLZ in addition to 30 % v/v CLZ EtOH solution was obtained to gain better interpretation. In addition, to assess the interaction of BHA+BHT and CLZ within selected three formulations, 30% v/v EtOH CLZ solution was used. We hypothesized that hydroethanolic solution used for micellar solution preparation probably could influence the antifungal activity, as EtOH itself is known to have antimicrobial property. Interestingly, when examined EtOH did not responded below MIC 1024, however, was found evident to promote antifungal property of plain CLZ in combination. The best three formulations were lately compared with respect to MIC values, where, CAT-3S showed promising activity against the clinical isolates. In particular, the calculated MIC values for CAT-3S was found to lie within the range of 0.25 – 8.0 (μg/ml) against FLZ / MLZ resistant and FLZ susceptible *C. albicans* isolates. Moreover the activity was promising against *C. tropicalis* isolates. Interestingly, all the three tested formulations were not found active against *C. glabrata* clinical isolates.

Given the fact that results suggested an interaction between CLZ and micellar encapsulated BHA+BHT, the FIC was calculated to investigate whether the combination was synergistic (SY), additive (AD), indifference (IN) or antagonistic (AG). This was carried out by FICI approach. Here, FICI represents the sum of FICs of each compound tested/ presented within the system (formulation), where, FIC is determined for each compound by dividing the MIC of each compound when used in combination by the MIC of each compound when used alone. Considering that FICI value among three screened formulations, CAT-3S was found with maximum number of synergism against 30 clinical isolates (Table 5). With regard to the FICI calculated values, CAT-3S was found to be most promising against FLZ resistant PDI/MDL54 clinical isolate with FICI = 0.13, therefore, the latter studies were performed against this clinical isolate. Results found in this *in vitro* experiment suggested a clear and

decisive role of the antioxidants as well as the micellar system. Moreover, MIC values revealed promising inhibition of the growth of *Candida* species at the concentration lower than the drug (CLZ). Therefore, *in vitro* antifungal activity showed CAT-3S was the best formulation among others which was thereafter accounted for further analysis and studies.

3.3. Morphological study

To gain more insight on the best scrutinized formulation i.e. CAT-3S, the morphological studies were performed. From the SEM images as presented in Fig. 4, it was well observed that CAT-3S was homogeneous with no signs of precipitation. Milky white appearance with a colloidal system characteristic was visualized. However, nano – micellar bodies were also visualized with uniform distribution within the gel matrix system. Importantly, in an attempt of preparing nanoemulsion, precipitation with formation of clumps was obtained, and thereafter bioadhesive polymeric system was taken into consideration. In addition, the image was also taken after duration of ~1 month (Fig. 4b) and after ~ 9 months (Fig. 4c) in order to visualize any morphological changes within the formulation, suggesting stability of CAT-3S for a period of ~ 9 month cycle. On the other hand, micellar structures were also characterized via SEM and TEM. Fig. 5, depicting spherical micellar formation with no structural transition, which can occur sometime due to presence of EtOH caused by compensation between electrostatic interaction and hydrophobic hydration. From TEM images (Fig. 5b,c) and physicochemical analysis, the size was found to be ~ 118 nm, with polydispersity index 0.17 ± 0.04 and zeta potential – 18.34 ± 2.43 mV suggesting narrow distribution and good stability of the micellar bodies within the system. In addition, it should be noted that carbomer molecule are negatively charged with tightly coiled structure therefore provided greater stability, which was well observed in the formulation.

The contact antifungal activity of CAT-3S was estimated using *C. albicans* (PGI/DML41) via TEM. To gain information with respect to contact activity and cytological damage caused by CAT-3S, the higher concentration i.e. 10 μg/ml was deliberately selected to avoid the budding of cells and cell adherence that are unaffected by the exposure. In addition single cell treatment has been presented to gain better understanding on the action on cell wall. From the images (Fig. 6), the morphological changes of *C. albicans* induced by treatment were clearly revealed by TEM. Fig. 6a of untreated *C. albicans* was well defined, intact shapes with smooth surface. After 15 min of treatment, a slight but considerable alteration was observed on fungal cell wall, whereas after 2 h and 6 h, well defined ultrastructural changes were noticed. Morphological cell wall deformation (peeling/ exfoliation) followed by shrinkage and complete cell damage was observed after 6 h (Fig. 6d). However, CLZ which is an imidazole derivative and known to act on fungal cell wall or membrane and binds to the heme part of cell wall leading to inhibition of ergosterol principally sterol in membrane and then destroys the integrity of the fungal membrane. In addition BHA and BHT do possess heme chelating property, so it is a speculation which might be possible that they might have acted in a same manner and provided synergism in order to get better antifungal drug action.

3.4. Stability studies

3.4.1. Photo-stability study

In general, there are no such scientific reports suggesting that CLZ is photolabile, the United States Pharmacopoeia and very few articles from Santos et al[40] recommends that photo protection of the drug during storage. In the present study, an examination was made to assess the ability of potential oxidation inhibitors (BHA/BHT) in prevention of CLZ photodegradation under UVC radiation. UVC is the shortest and highest energy UV with

wavelengths less than 290 nm and being shortest is the most damaging types of UV radiations. After 14 h exposure, the samples were analyzed for amount of remaining CLZ. The presented Fig. 7 shows the photodegradation of methanolic solution of CLZ and CAT-3S in comparison to the dark control of the CLZ. Form the results, the CLZ concentration of dark control was found almost 100%, whereas, methanolic CLZ solution showed significant degradation of 76%. In comparison to dark control, the formulation (CAT-3S) resist with degradation of 22%. The result showed that antioxidants present in CAT-3S led to an increase of approximately 3.5 times of exposed methanolic solution of CLZ. The enhanced photostability is well attributed to the standard antioxidants. It can be explained as likely antioxidants might have prevented the degradation caused by UV exposure by absorbing the UV radiations or by trapping the free radicals generated during the process of oxidation [41, 42].

3.4.2. Physical stability

In 9 month stability cycle at room temperature and light protected, no changes were observed in appearance, with no color change and without any kind of precipitation (Fig. 4c). Whist in 60 days, marginal decrease was found in cumulative % drug release and pH. In addition, viscosity was also found to decrease marginally which might be because of EtOH presence in the formulation, thus, affecting the spreadability. With regard to BHA+BHT loaded micellar particle size and zeta potential, they were reasonably steady with slight increase in size and decrease in charge (Fig. 8). In addition, polydispersity index was also found with marginal decrease.

3.5. Skin irritation and in vivo toxicity study

Conventional therapy is associated with visual noticeable skin irritation check. If observed, it strongly restricts the applicability and acceptability of topical formulation by the patients. Ideally, the developed formulation should not cause any kind of irritation marks. In present investigation, skin irritation studies suggested that CAT-3S exhibited considerably no

irritation. The primary irritation index (PII) was found to be 0.00, reflecting no irritation within the limited duration of studied time. In addition, no erythema or edema was observed on the abraded rat skin when compared with control (without treatment).

However, going beyond the conventional therapy evaluation and gain much clear perspective, we intended to examine the *in vivo* toxicity within the major organs. The photo-micrographs of skin histological sections of treated and untreated animals are shown in Fig. 9. H and E stained sections of control skin sample showed epidermis consisting of a cornified squamous layer and underlying germinative layer. No inflammatory infiltrate, granulomatous evidence of malignancy was visualized. The formulation CAT-3S did not show sign of inflammation such as inflammatory infiltrate or edema. Compared to the control, no histopathological changes were visualized in other major organs (liver, kidney, and intestine) in treated animals. These results revealed that the developed surfactant aided antioxidants within CLZ gel system is safe for topical delivery.

3.6. Confocal laser scanning microscopy

Rhodamine B is an amphoteric dye, although usually listed as basic as it has an overall positive charge. On the other hand, carbopol polymer is anionic in nature, thus generates negative charges along their backbone and has the efficiency to bind with positively charged moiety via ion-ion interactions [43]. Employing CLSM [36, 44] of rat skin, the penetration of the dye within gel was investigated in order to assess the penetration range. The results of the study demonstrated that the penetration and accumulation within epidermis section of skin (Fig. 10). It can be concluded that system having surfactant aided antioxidant micellar system provides an extra driving force to the molecules present in carbopol gel base, as well as allowing better penetration by destabilizing the membrane. On the other side, ethanolic solution of drug was found to accumulate in the stratum corneum only. The study suggesting

the relevance of residence time for drug on infected site offered by three dimensional polymeric gel system.

3.7. In vivo antifungal study (mouse model)

The *in vivo* antifungal activity of plain CLZ formulation and developed formulation CAT-3S (1 mg/cm^2 and 5 mg/cm^2) was determined by challenging the animals with FLZ resistant *C. albicans* (PGI/DML54) on 8 days mouse model. From Fig. 11, it was found that infection in all animals was well established. The efficacy of the formulation CAT-3S was assessed on the basis of viable CFU count at different time intervals after treatment. Results revealed that CAT-3S possessed significant therapeutic efficacy, as compared to plain drug. After three days both CAT-3S and plain CLZ formulation significantly reduced the growth of *C. albicans*. Interestingly, at dose level of 1 mg/cm^2 plain CLZ formulation exhibits somewhat higher efficacy than CAT-3S with 2.14 $\log_{10}$ reduction in viable CFU (**$p<0.01$; Fig.) of *C. albicans* when compared with 48 h control. At the same time, formulation CAT-3S at dose level of 5 mg/cm^2 produced 2.28 $\log_{10}$ reduction in viable CFU (**$p<0.01$; Fig.) of *C. albicans* when compared with 48 h control. However, this positive effect of plain CLZ formulation did not maintained throughout the experiment as increment in the viable CFUs was observed on day 5, 6, 7, and 8. In contrast to this, CAT-3S constantly reduced the burden of viable CFUs of infecting organism and appreciated the longer term reduction of fungal infection in skin. In particular, CAT-3S induced 3.26, 3.58, 4.20, and 4.65 $\log_{10}$ reduction in viable CFUs of *C. albicans* on day 5, 6, 7, and 8 respectively when compared with 48 h control. Similarly, formulation at 5 mg/cm^2 decreased the burden of *C. albicans* by 4.52, 4.81, 5.38, and 5.73 $\log_{10}$ when growth was observed after 5, 6, 7, and 8 days respectively. It was further interesting to note that on day 8 numbers of viable CFUs was increased to 7.11 $\log_{10}$. As it can be clearly stated that the animals treated with CAT-3S, demonstrated low fungal burden in skin with a colony count significantly less abundant than those treated with

plain CLZ formulation. This impact of CAT-3S can be explained in term of presence of BHA and BHT within SDS hydroethanolic micellar system in bioadhesive gel, providing longer residence time, higher bioavailability with synergistic effect offered by antioxidants.

Conclusion

For the first time, based on thermodynamic analysis the present study showed the feasibility and compatibility of utilizing antioxidant micellar system in combination of standard antifungal topical formulation. Conclusively, the developed formulation had satisfactory qualities. The results obtained in the present study showed that the formulated gel holds good bioadhesive property, stability, prolonged residence time and higher penetration. In addition physicochemical studies directed the utilization of thermodynamically stable hydroethanolic antioxidant's micellar system, which showed potential synergism with better antifungal profile. From *in vitro* results, CAT-3S formulation was found to be the most promising one among all formulations. Biophysical morphology study revealed the mechanistic approach of CAT-3S via initial exfoliation causing drug accumulation and lastly cell damage. The fungal cell damage was well defined on the changes of morphology and biophysical properties. Photostability study suggested potential role of antioxidants to prevent the drug degradation caused by UV exposure. *In vivo* study demonstrated low fungal burden in skin with a colony count significantly less abundant with CAT-3S, than those treated with plain CLZ formulation.

Acknowledgements

Authors, V. Bhardwaj and P. Sharma thank DST, New Delhi for financial assistance in the form of major project (Grant. No. SR/FT/CS-59/2009); Institute of Microbial Technology, Chandigarh; Medical Microbiology Department, Postgraduate Institute of Medical Education and Research, Chandigarh and Indra Gandhi Medical College, Shimla (H.P.) India, for

supporting the study with clinical isolates, and NIPER, Mohali, India for providing sample analysis support.

References

1. D. J. McLaughlin, D. S. Hibbett, F. Lutzoni, J. W. Spatafora and R. Vilgalys, *Trends in Microbiology*, 2009, 17, 488-497.
2. R. G. Dalziel, J. R. Fitzgerald, C. A. Mims, A. A. Nash and J. Stephen, *Mims' pathogenesis of infectious disease*, Academic Press, 2000.
3. W. R. Jarvis, *Clinical Infectious Diseases*, 1995, 20, 1526-1530.
4. M. Ameen, *Clinics in dermatology*, 2010, 28, 197-201.
5. J. Kim and P. Sudbery, *The Journal of Microbiology*, 2011, 49, 171-177.
6. H. V. Bossche, in *Current Topics in Medical Mycology*, Springer, 1985, 313-351.
7. W. H. Organization, *The Selection and Use of Essential Medicines: Report of the WHO Expert Committee, 2005 (including the 14th Model List of Essential Medicines)*, World Health Organization, 2006.
8. W. Yang, N. P. Wiederhold and R. O. Williams III, 2008.
9. S. Jana, S. Manna, A. K. Nayak, K. K. Sen and S. K. Basu, *Colloids and Surfaces B: Biointerfaces*, 2014, 114, 36-44.
10. J. Boujlel and P. Coussot, *Soft Matter*, 2013, 9, 5898-5908.
11. M. Ravi Kumar, *Drug Discovery Today*, 2012, 17, 407-408.
12. C. Caddeo, M. Manconi, A. M. Fadda, F. Lai, S. Lampis, O. Diez-Sales and C. Sinico, *Colloids and Surfaces B: Biointerfaces*, 2013, 111, 327-332.
13. R. Motheram and G. C. Williams, US Patent 8,658,676, 2014.
14. R. W. Weber, *Food Allergy: Adverse Reaction to Foods and Food Additives*, 2013, 393.
15. J. Liu and L. Li, *European Journal of Pharmaceutical Sciences*, 2005, 25, 237-244.

16. Y. Zhang, H. F. Chan and K. W. Leong, *Advanced Drug Delivery Reviews*, 2013, 65, 104-120.

17. V. Bhardwaj, S. Chauhan, K. Sharma and P. Sharma, *Thermochimica Acta*, 2014, 577, 66-78.

18. V. Bhardwaj, S. Chauhan and P. Sharma, *Fluid Phase Equilibria*, 2014, 373, 63-71.

19. V. Bhardwaj, P. Sharma, M. Chauhan and S. Chauhan, *Journal of Molecular Liquids*, 2013, 180, 192-199.

20. V. Bhardwaj, P. Sharma and S. Chauhan, *Thermochimica Acta*, 2013, 566, 155-161.

21. P. Sharma, V. Bhardwaj, T. Chaudhary, I. Sharma, P. Kumar and S. Chauhan, *Journal of Molecular Liquids*, 2013, 187, 287-293.

22. V. Bhardwaj, T. Bhardwaj, K. Sharma, A. Gupta, S. Chauhan, S. S. Cameotra, S. Sharma, R. Gupta and P. Sharma, *RSC Advances*, 2014, 4, 24935-24943.

23. M. Fresno, A. Ramírez and M. Jiménez, *European Journal of Pharmaceutics and Biopharmaceutics*, 2002, 54, 329-335.

24. P. Mura, F. Maestrelli, M. L. González-Rodríguez, I. Michelacci, C. Ghelardini and A. M. Rabasco, *European Journal of Pharmaceutics and Biopharmaceutics*, 2007, 67, 86-95.

25. R. Ekiert, J. Krzek and P. Talik, *Talanta*, 2010, 82, 1090-1100.

26. Y. N. Kalia and R. H. Guy, *Advanced Drug Delivery Reviews*, 2001, 48, 159-172.

27. J. P. Jain and N. Kumar, *European Journal of Pharmaceutical Sciences*, 2010, 40, 456-465.

28. A. Espinel-Ingroff, A. Fothergill, M. Ghannoum, E. Manavathu, L. Ostrosky-Zeichner, M. Pfaller, M. Rinaldi, W. Schell and T. Walsh, *Journal of Clinical Microbiology*, 2005, 43, 5243-5246.

29. R. Cruz, S. Werneck, C. Oliveira, P. Santos, B. Soares, D. Santos and P. Cisalpino, *Journal of Clinical Microbiology*, 2012, 02231-02212.

30. A. Aller, E. Martin-Mazuelos, F. Lozano, J. Gomez-Mateos, L. Steele-Moore, W. Holloway, M. Gutierrez, F. Recio and A. Espinel-Ingroff, *Antimicrobial Agents and Chemotherapy*, 2000, 44, 1544-1548.

31. M. D. Johnson, C. MacDougall, L. Ostrosky-Zeichner, J. R. Perfect and J. H. Rex, *Antimicrobial Agents and Chemotherapy*, 2004, 48, 693-715.

32. K. S. Kim, Y.-S. Kim, I. Han, M.-H. Kim, M. H. Jung and H.-K. Park, *PLoS ONE*, 2011, 6, e28176.

33. R. K. Basniwal, H. S. Buttar, V. Jain and N. Jain, *Journal of Agricultural and Food Chemistry*, 2011, 59, 2056-2061.

34. S. D. Mandawgade and V. B. Patravale, *International Journal of Pharmaceutics*, 2008, 363, 132-138.

35. S. Khurana, N. Jain and P. Bedi, *Life Sciences*, 2013, 92, 383-392.

36. P. Verma and K. Pathak, *Nanomedicine: Nanotechnology, Biology and Medicine*, 2012, 8, 489-496.

37. K. Maebashi, T. Itoyama, K. Uchida, N. Suegara and H. Yamaguchi, *Medical Mycology*, 1994, 32, 349-359.

38. M. M. Abdel-Mottaleb, N. Mortada, A. El-Shamy and G. Awad, *Drug Development and Industrial Pharmacy*, 2009, 35, 311-320.

39. M. Ning, Y. Guo, H. Pan, X. Chen and Z. Gu, *Drug Development and Industrial Pharmacy*, 2005, 31, 375-383.

40. S. S. Santos, A. Lorenzoni, L. M. Ferreira, J. Mattiazzi, A. I. Adams, L. B. Denardi, S. H. Alves, S. R. Schaffazick and L. Cruz, *Materials Science and Engineering: C*, 2013, 33, 1389-1394.

41. S. S. Santos, A. Lorenzoni, N. S. Pegoraro, L. B. Denardi, S. H. Alves, S. R. Schaffazick and L. Cruz, *Colloids and Surface B: Biointerfaces,*2014, 116, 270-276.

42. A. M. Mariana, Y. B. Man, S. A. Nazimah, and I. Amin, *International Journal of Food Sciences and Nutrition,*2009, 60, 114-123.

43. R. Barreiro-Iglesias, C. Alvarez-Lorenzo and A. Concheiro, *Journal of Controlled Release*, 2001, 77, 59-75.

44. S. Khurana, N. K. Jain, and P. M. S. Bedi, *Life Sciences,* 2013, 92, 383-392.

Figure Captions

Fig. 1. Chemical structures; i) Clotrimazole, ii) Butylated hydroxyanisole (BHA), iii) Butylated hydroxytoluene (BHT), iv) Anionic surfactant: sodium dodecyl sulfate (SDS), v) Cationic surfactant: Cetyltrimethylammonium bromide (CTAB), and vi) Nonionic surfactant: *tert*-octylphenol ethoxylate (Triton X-100).

Fig. 2. FTIR representing drug-polymer compatibility; (a) carbopol 940, (b) clotrimazole and (c) carbopol+clotrimazole.

Fig. 3. Plot representing % cumulative drug release as function of time, where C denotes CLZ; A denotes BHA, T denotes BHT; S denotes SDS; C denotes CTAB and X denotes TX100.

Fig. 4. Scanning electron microscopy images of formulation (CAT-3S); (a) after preparation, (b) after ~ 1 month, and (c) after ~ 9 months.

Fig. 5. (a) Scanning electron microscopy image of prepared micelles, (b, c) transmission electron microscopy images of micelle dispersed within the formulation CAT-3S.

Fig. 6. TEM images of an unexposed (control) cell and CAT-3S (10 μg/ml) treated cell of *C. albicans*.

Fig. 7. Plot representing clotrimazole (CLZ) content after 14 h exposure to UV radiations.

Fig. 8. pH, particle size (nm), polydispersity and zeta potential (mV) of micellar structure, after preparation and after 60 days.

Fig. 9. Histological images of major organs (A) untreated and (B) formulation (CAT-3S) treated, suggesting no toxicity.

Fig. 10. Confocal laser scanning micrograph of rat skin (A) treatment with hydroalcoholic solution of Rhodamine B, and (B) CAT-3S (Rhodamine B in polymeric system).

Figure. 11. *In vivo* antifungal activity representing the infection burden in 8 days mouse model.

List of Tables

Table 1 Data representing the ingredient concentrations utilized in gel formulations.

S. No.	Codes	CLZ (%)	BHA (mg)	BHT (mg)	SDS (mg)	CTAB (mg)	TX100 (mg)
1	CA-1S	1	5	-	17	-	-
2	CA-2S	1	5	-	20	-	-
3	CA-3S	1	5	-	23	-	-
4	CT-1S	1	-	4	17	-	-
5	CT-2S	1	-	4	20	-	-
6	CT-3S	1	-	4	23	-	-
7	CAT-1S	1	5	4	17	-	-
8	CAT-2S	1	5	4	20	-	-
9	CAT-3S	1	5	4	23	-	-
10	CA-1C	1	5	-	-	3	-
11	CA-2C	1	5	-	-	4	-
12	CA-3C	1	5	-	-	4.5	-
13	CT-1C	1	-	4	-	3	-
14	CT-2C	1	-	4	-	4	-
15	CT-3C	1	-	4	-	4.5	-
16	CAT-1C	1	5	4	-	3	-
17	CAT-2C	1	5	4	-	4	-
18	CAT-3C	1	5	4	-	4.5	-
19	CA-1X	1	5	-	-	-	1
20	CA-2X	1	5	-	-	-	2
21	CA-3X	1	5	-	-	-	3
22	CT-1X	1	-	4	-	-	1
23	CT-2X	1	-	4	-	-	2
24	CT-3X	1	-	4	-	-	3
25	CAT-1X	1	5	4	-	-	1
26	CAT-2X	1	5	4	-	-	2
27	CAT-3X	1	5	4	-	-	3

CLZ = Clotrimazole; **CA**= CLZ+BHA; **CT**= CLZ+BHT; **CAT**= CLZ+BHA+BHT; **S**= SDS; **C**= CTAB; **X**= TX100

Table 2 Different release models employed and their equation.

Model	**Equation**
Zero order	$Q_t = Q_0 + Kt$
First order	$ln\ Q_t = ln\ Q_0 + Kt$
Higuchi	$Q_t = K_H t^{1/2}$
Korsmeyer-Peppas	$Q_t / Q_\infty = Kt^n$ $(n = 0.5, 0.75, 1.25)$

Where, Q_t is the amount of drug released in time t, Q_∞ is the initial amount of drug and K is release rate constants of respective equations, respectively.

Table 3 Physicochemical characterization data representing pH, viscosity, drug release, and spreadability.

S. No.	Codes	pH	Viscosity (cP)	Cumulative % drug release (6h)	Spreadability (g.cm/s)
1	CA-1S	6.9	46884 ± 24	82.44 ± 0.52	12.53 ± 0.15
2	CA-2S	6.8	46719 ± 19	87.23 ± 0.36	14.75 ± 0.21
3	CA-3S	7.1	47839 ± 27	94.33 ± 0.60	14.00 ± 0.32
4	CT-1S	6.9	46738 ± 25	82.74 ± 0.26	12.75 ± 0.13
5	CT-2S	7.2	46814 ± 18	87.63 ± 0.43	13.75 ± 0.17
6	CT-3S	6.8	47473 ± 31	94.63 ± 0.31	13.15 ± 0.22
7	CAT-1S	6.8	47249 ± 22	83.82 ± 0.44	14.33 ± 0.16
8	CAT-2S	7.0	47399 ± 20	88.40 ± 0.29	13.33 ± 0.23
9	CAT-3S	7.2	47392 ± 37	95.68 ± 0.50	14.85 ± 0.34
10	CA-1C	6.9	46984 ± 30	79.02 ± 0.34	13.53 ± 0.12
11	CA-2C	7.3	47008 ± 29	81.33 ± 0.42	14.33 ± 0.14
12	CA-3C	6.8	46953 ± 18	83.95 ± 0.54	14.03 ± 0.25
13	CT-1C	7.0	46896 ± 36	79.49 ± 0.57	13.52 ± 0.19
14	CT-2C	7.2	47255 ± 28	81.82 ± 0.31	13.64 ± 0.11
15	CT-3C	6.9	46949 ± 31	84.47 ± 0.30	12.53 ± 0.18
16	CAT-1C	7.1	47391 ± 40	81.05 ± 0.48	14.15 ± 0.27
17	CAT-2C	6.9	47195 ± 27	82.21 ± 0.35	14.53 ± 0.20
18	CAT-3C	6.8	46849 ± 35	85.18 ± 0.43	13.75 ± 0.17
19	CA-1X	7.3	46988 ± 36	85.92 ± 0.26	13.53 ± 0.29
20	CA-2X	7.0	47105 ± 25	88.82 ± 0.35	13.33 ± 0.33
21	CA-3X	7.2	46966 ± 31	93.38 ± 0.25	13.53 ± 0.16
22	CT-1X	6.9	47227 ± 29	86.14 ± 0.36	13.85 ± 0.23
23	CT-2X	7.1	47310 ± 34	89.07 ± 0.29	14.00 ± 0.17
24	CT-3X	6.8	46794 ± 30	94.00 ± 0.42	13.75 ± 0.26
25	CAT-1X	6.9	47399 ± 23	87.05 ± 0.52	14.15 ± 0.18
26	CAT-2X	7.3	47118 ± 28	89.50 ± 0.46	13.45 ± 0.21
27	CAT-3X	7.1	47284 ± 27	94.98 ± 0.23	13.70 ± 0.33

CA= CLZ+BHA; **CT**= CLZ+BHT; **CAT**= CLZ+BHA+BHT; **S**= SDS; **C**= CTAB; **X**= TX100

Table 4 *In vitro* release rate profile with model kinetics for best three formulations.

Formulations	Zero order		First order		Higuchi		Korsmeyer–Peppas	
	R^2	K	R^2	K	R^2	K	R^2	n
CAT-3S	0.956	0.231	0.506	0.001	0.986	4.637	0.972	0.33
CAT-3C	0.997	0.227	0.693	0.001	0.929	4.637	0.994	0.32
CAT-3X	0.995	0.252	0.653	0.001	0.942	5.207	0.995	0.33

CAT= CLZ+BHA+BHT; **S**= SDS; **C**= CTAB; **X**= TX100

Table 5 Antifungal activity (MIC μg/ml) of CAT-3S formulation against various *Candida* species clinical isolates.

S. No.	Clinical Isolates	Type	Species	CAT-3S	BHA	BHT	FLZ	CLZ	FICI	RESULT
1	PGI/DML14	R	*C. albicans*	0.50	>512	64	>512	2.0	0.26	SY
2	PGI/DML34	R	*C. albicans*	1.0	>512	128	>512	2.0	0.51	AD
3	PGI/DML41	R	*C. albicans*	0.25	256	64	32	1.0	0.26	SY
4	PGI/DML54	R	*C. albicans*	0.50	>512	128	>512	4.0	0.13	SY
5	PGI/DML61	R	*C. albicans*	8.0	>512	>512	128	32	0.28	SY
6	PGI/DML85	R	*C. albicans*	8.0	>512	>512	>512	32	0.28	SY
7	PGI/DML43A	R	*C. albicans*	2.0	256	256	64	8.0	0.27	SY
8	PGI/DML77A	R	*C. albicans*	2.0	>512	>512	>512	16	0.13	SY
9	PGI/DML94A	R	*C. albicans*	16	>512	>512	>512	32	0.56	AD
10	PGI/DML106A	R	*C. albicans*	0.50	128	32	16	2.0	0.27	SY
11	PGI/DML05C	R	*C. albicans*	4.0	>512	128	64	8.0	0.54	AD
12	PGI/DML83C	R	*C. albicans*	1.0	256	64	>512	4.0	0.27	SY
13	PGI/DML74E	R	*C. albicans*	0.25	256	64	32	2.0	0.13	SY
14	PGI/DML88E	R	*C. albicans*	1.0	>512	128	>512	4.0	0.26	SY
15	PGI/DML92E	R	*C. albicans*	0.50	>512	64	>512	4.0	0.13	SY
16	PGI/DSS103	S	*C. albicans*	0.25	256	128	128	4.0	0.07	SY
17	PGI/DSS114	S	*C. albicans*	0.50	>512	128	256	8.0	0.07	SY
18	PGI/DSS123	S	*C. albicans*	4.0	128	>512	>512	16	0.31	SY
19	IGMC/LM1/021	S	*C. tropicalis*	0.50	>512	128	64	1.0	0.51	AD
20	IGMC/LM1/025	S	*C. tropicalis*	0.50	>512	32	>512	4.0	0.15	SY
21	IGMC/LM1/044	S	*C. tropicalis*	2.0	>512	128	32	4.0	0.52	AD
22	IGMC/LM2/010	S	*C. tropicalis*	1.0	256	>512	128	2.0	0.51	AD
23	IGMC/LM2/004	S	*C. tropicalis*	4.0	>512	64	64	4.0	1.07	IN
24	IGMC/LM2/001	S	*C. tropicalis*	8.0	128	>512	256	16	0.58	AD
25	IGMC/LM2/033	S	*C. tropicalis*	2.0	>512	128	64	8.0	0.27	SY
26	IGMC/LM4A/05	S	*C. tropicalis*	4.0	256	32	256	4.0	1.14	IN
27	IGMC/LM1/070	S	*C. glabrata*	4.0	256	64	16	0.50	8.08	AN
28	IGMC/LM1/091	S	*C. glabrata*	8.0	>512	32	128	2.0	4.27	AN
29	IGMC/LM4A/12	S	*C. glabrata*	16	>512	>512	>512	8.0	2.06	IN
30	IGMC/LM4A/19	S	*C. glabrata*	8.0	128	256	256	2.0	4.09	AN

Table 6 Antifungal activity (MIC μg/ml) of CAT-3C formulation against various *Candida* species clinical isolates.

S. No.	Clinical Isolates	Type	Species	CAT-3C	BHA	BHT	FLZ	CLZ	FICI	RESULT
1	PGI/DML14	R	*C. albicans*	1.0	>512	64	>512	2.0	0.52	AD
2	PGI/DML34	R	*C. albicans*	1.0	>512	128	>512	2.0	0.51	AD
3	PGI/DML41	R	*C. albicans*	1.0	256	64	32	1.0	1.02	IN
4	PGI/DML54	R	*C. albicans*	1.0	>512	128	>512	4.0	0.26	SY
5	PGI/DML61	R	*C. albicans*	8.0	>512	>512	128	32	0.28	SY
6	PGI/DML85	R	*C. albicans*	16	>512	>512	>512	32	0.06	SY
7	PGI/DML43A	R	*C. albicans*	4.0	256	256	64	8.0	0.53	AD
8	PGI/DML77A	R	*C. albicans*	8.0	>512	>512	>512	16	0.53	AD
9	PGI/DML94A	R	*C. albicans*	16	>512	>512	>512	32	0.56	AD
10	PGI/DML106A	R	*C. albicans*	1.0	128	32	16	2.0	0.54	AD
11	PGI/DML05C	R	*C. albicans*	4.0	>512	128	64	8.0	0.54	AD
12	PGI/DML83C	R	*C. albicans*	1.0	256	64	>512	4.0	0.27	SY
13	PGI/DML74E	R	*C. albicans*	1.0	256	64	32	2.0	0.52	AD
14	PGI/DML88E	R	*C. albicans*	1.0	>512	128	>512	4.0	0.26	SY
15	PGI/DML92E	R	*C. albicans*	0.50	>512	64	>512	4.0	0.13	SY
16	PGI/DSS103	S	*C. albicans*	0.25	256	128	128	4.0	0.07	SY
17	PGI/DSS114	S	*C. albicans*	1.0	>512	128	256	8.0	0.14	SY
18	PGI/DSS123	S	*C. albicans*	4.0	128	>512	>512	16	0.29	SY
19	IGMC/LM1/021	S	*C. tropicalis*	0.50	>512	128	64	1.0	0.51	AD
20	IGMC/LM1/025	S	*C. tropicalis*	1.0	>512	32	>512	4.0	0.28	SY
21	IGMC/LM1/044	S	*C. tropicalis*	4.0	>512	128	32	4.0	1.04	IN
22	IGMC/LM2/010	S	*C. tropicalis*	2.0	256	>512	128	2.0	1.01	IN
23	IGMC/LM2/004	S	*C. tropicalis*	2.0	>512	64	64	4.0	0.54	AD
24	IGMC/LM2/001	S	*C. tropicalis*	8.0	128	>512	256	16	0.58	AD
25	IGMC/LM2/033	S	*C. tropicalis*	2.0	>512	128	64	8.0	0.27	SY
26	IGMC/LM4A/05	S	*C. tropicalis*	1.0	256	32	256	4.0	0.29	SY
27	IGMC/LM1/070	S	*C. glabrata*	1.0	256	64	16	0.50	2.02	IN
28	IGMC/LM1/091	S	*C. glabrata*	1.0	>512	32	128	2.0	0.54	AD
29	IGMC/LM4A/12	S	*C. glabrata*	8.0	>512	>512	>512	8.0	1.03	IN
30	IGMC/LM4A/19	S	*C. glabrata*	2.0	128	256	256	2.0	1.02	IN

Table 7 Antifungal activity (MIC μg/ml) of CAT-3X formulation against various *Candida* species clinical isolates.

S. No.	Clinical Isolates	Type	Species	CAT-3X	BHA	BHT	FLZ	CLZ	FICI	RESULT
1	PGI/DML14	R	*C. albicans*	0.50	>512	64	>512	2.0	0.26	SY
2	PGI/DML34	R	*C. albicans*	0.50	>512	128	>512	2.0	0.26	SY
3	PGI/DML41	R	*C. albicans*	0.25	256	64	32	1.0	0.26	SY
4	PGI/DML54	R	*C. albicans*	1.0	>512	128	>512	4.0	0.26	SY
5	PGI/DML61	R	*C. albicans*	8.0	>512	>512	128	32	0.28	SY
6	PGI/DML85	R	*C. albicans*	16	>512	>512	>512	32	0.56	AD
7	PGI/DML43A	R	*C. albicans*	2.0	256	256	64	8.0	0.27	SY
8	PGI/DML77A	R	*C. albicans*	4.0	>512	>512	>512	16	0.27	SY
9	PGI/DML94A	R	*C. albicans*	16	>512	>512	>512	32	0.56	AD
10	PGI/DML106A	R	*C. albicans*	0.50	128	32	16	2.0	0.27	SY
11	PGI/DML05C	R	*C. albicans*	2.0	>512	128	64	8.0	0.27	SY
12	PGI/DML83C	R	*C. albicans*	2.0	256	64	>512	4.0	0.54	AD
13	PGI/DML74E	R	*C. albicans*	1.0	256	64	32	2.0	0.52	AD
14	PGI/DML88E	R	*C. albicans*	2.0	>512	128	>512	4.0	0.52	AD
15	PGI/DML92E	R	*C. albicans*	1.0	>512	64	>512	4.0	0.27	SY
16	PGI/DSS103	S	*C. albicans*	0.50	256	128	128	4.0	0.13	SY
17	PGI/DSS114	S	*C. albicans*	2.0	>512	128	256	8.0	0.27	SY
18	PGI/DSS123	S	*C. albicans*	2.0	128	>512	>512	16	0.15	SY
19	IGMC/LM1/021	S	*C. tropicalis*	0.50	>512	128	64	1.0	0.51	AD
20	IGMC/LM1/025	S	*C. tropicalis*	1.0	>512	32	>512	4.0	0.28	SY
21	IGMC/LM1/044	S	*C. tropicalis*	2.0	>512	128	32	4.0	0.52	AD
22	IGMC/LM2/010	S	*C. tropicalis*	1.0	256	>512	128	2.0	0.51	AD
23	IGMC/LM2/004	S	*C. tropicalis*	4.0	>512	64	64	4.0	1.07	IN
24	IGMC/LM2/001	S	*C. tropicalis*	8.0	128	>512	256	16	0.58	AD
25	IGMC/LM2/033	S	*C. tropicalis*	2.0	>512	128	64	8.0	0.27	SY
26	IGMC/LM4A/05	S	*C. tropicalis*	1.0	256	32	256	4.0	0.29	SY
27	IGMC/LM1/070	S	*C. glabrata*	2.0	256	64	16	0.50	4.04	AN
28	IGMC/LM1/091	S	*C. glabrata*	1.0	>512	32	128	2.0	0.53	AD
29	IGMC/LM4A/12	S	*C. glabrata*	16	>512	>512	>512	8.0	2.06	IN
30	IGMC/LM4A/19	S	*C. glabrata*	8.0	128	256	256	2.0	4.13	AN

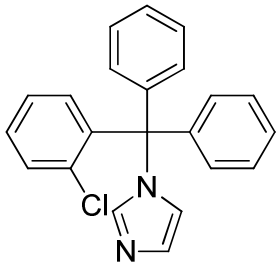

i) Clotrimazole

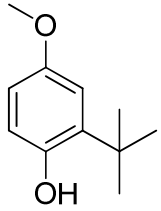

ii) Butylated Hydroxyanisle

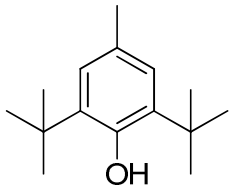

iii) Butylated Hydroxytoluene

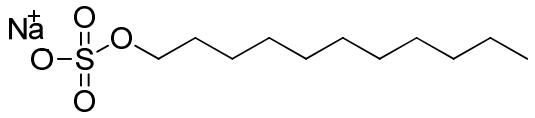

iv) Anionic surfactant: Sodium dodecyl sulfate (SDS)

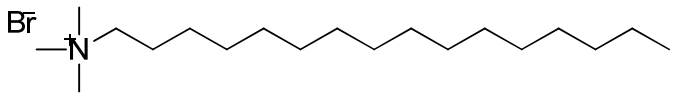

v) Cationic surfactant: Cetyltrimethylammonium bromide (CTAB)

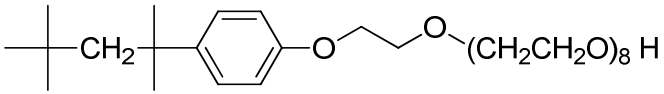

vi) Nonionic surfactant: *tert*-octylphenol ethoxylate (Triton X - 100)

Fig. 1. Chemical structures; i) Clotrimazole, ii) Butylated hydroxyanisole (BHA), iii) Butylated hydroxytoluene (BHT), iv) Anionic surfactant: sodium dodecyl sulfate (SDS), v) Cationic surfactant: Cetyltrimethylammonium bromide (CTAB), and vi) Nonionic surfactant: *tert*-octylphenol ethoxylate (Triton X-100).

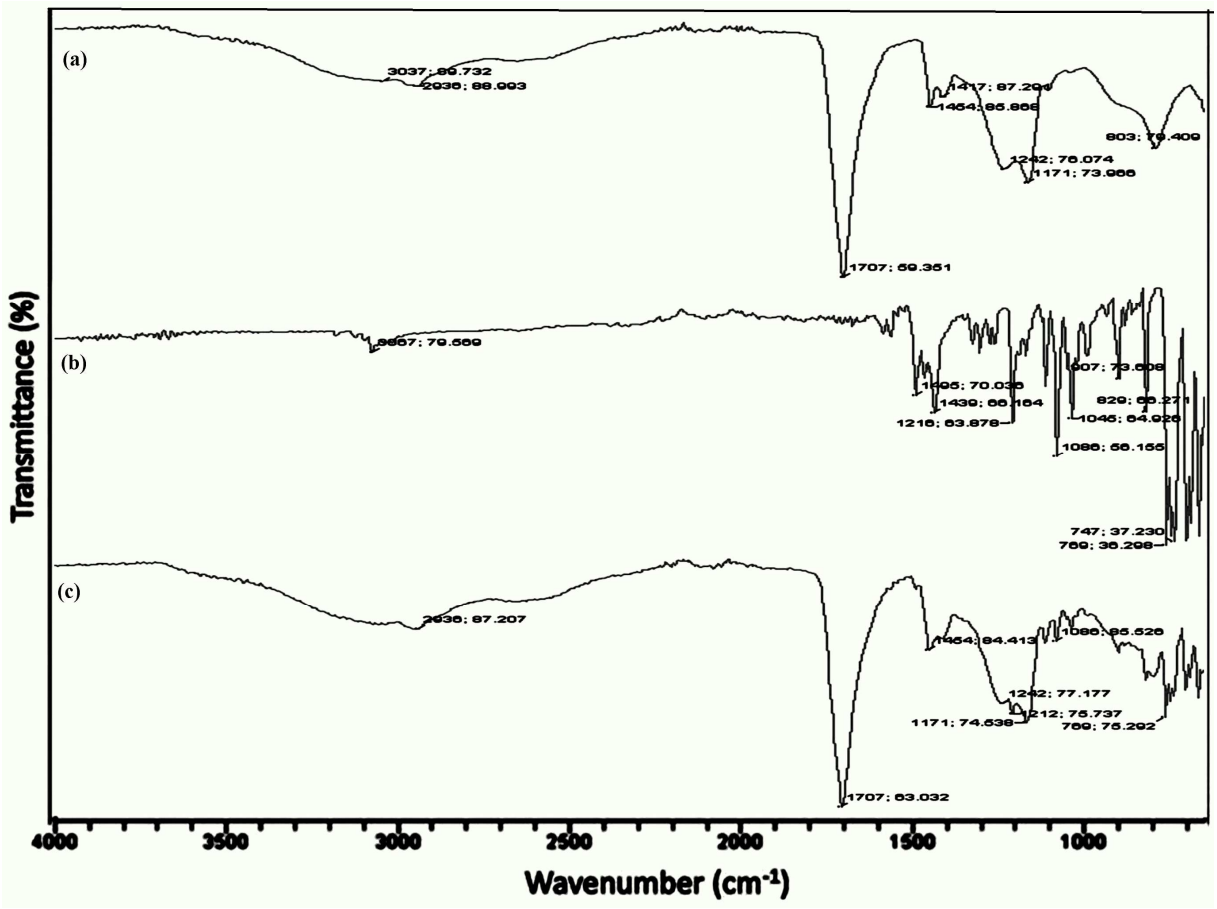

Fig. 2. FTIR representing drug-polymer compatibility; (a) carbopol 940, (b) clotrimazole and (c) carbopol+clotrimazole.

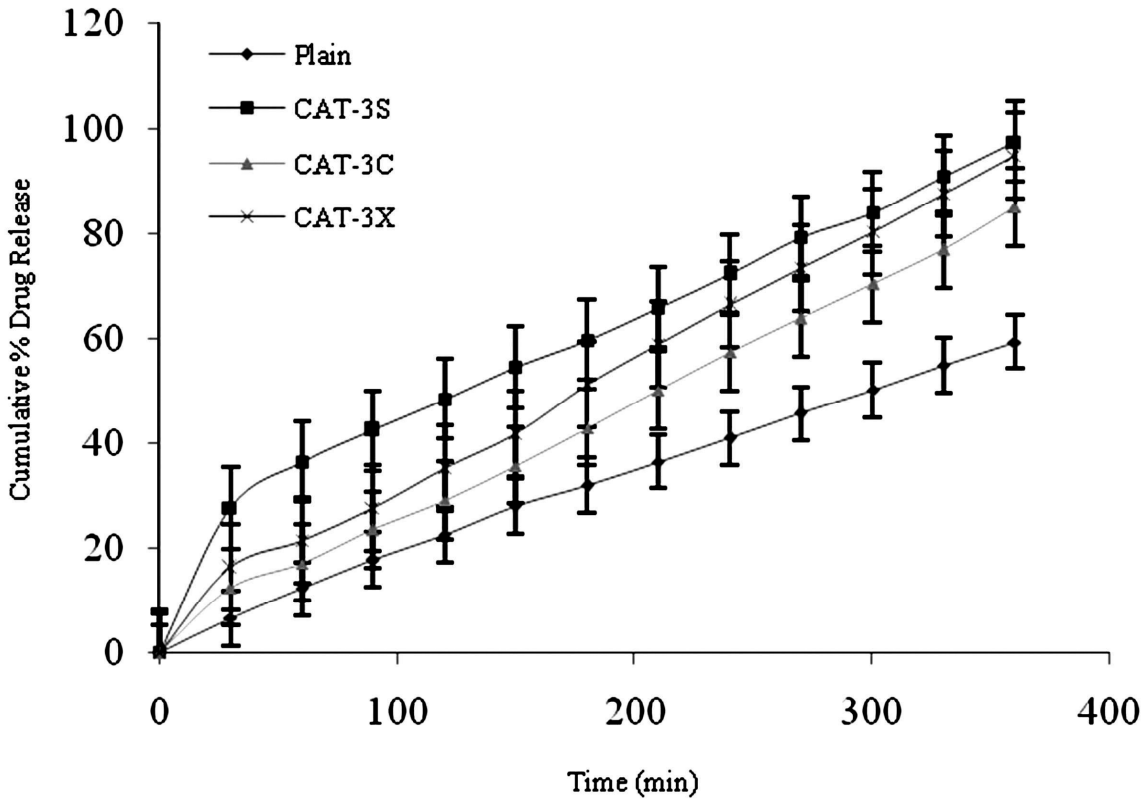

Fig. 3. Plot representing % cumulative drug release as function of time, where C denotes CLZ; A denotes BHA, T denotes BHT; S denotes SDS; C denotes CTAB and X denotes TX100.

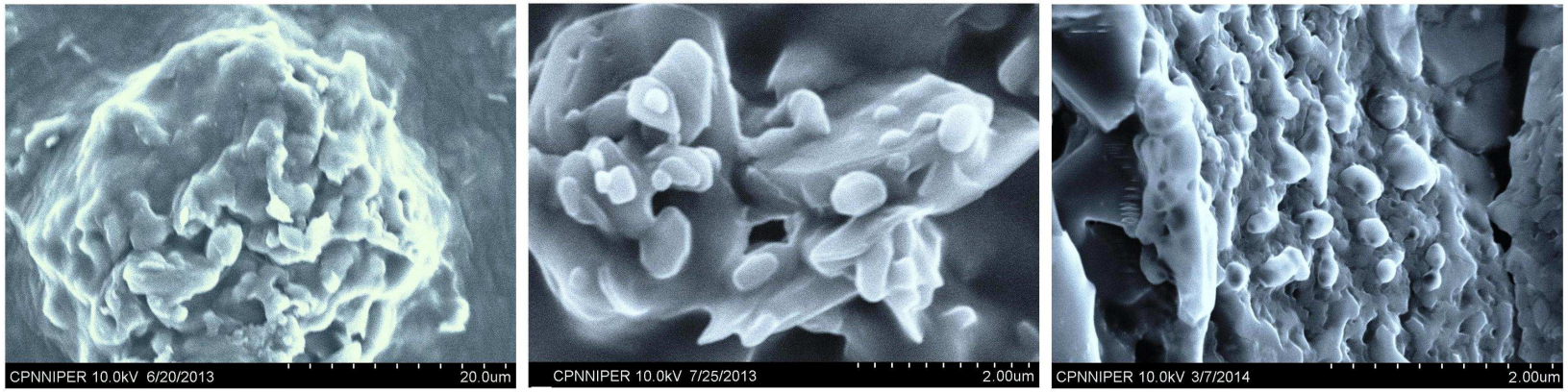

(a) **After preparation** (b) **After ~ 1 month** (c) **After ~ 9 month**

Fig. 4. Scanning electron microscopy images of formulation (CAT-3S); (a) after preparation, (b) after ~ 1 month, and (c) after ~ 9 months.

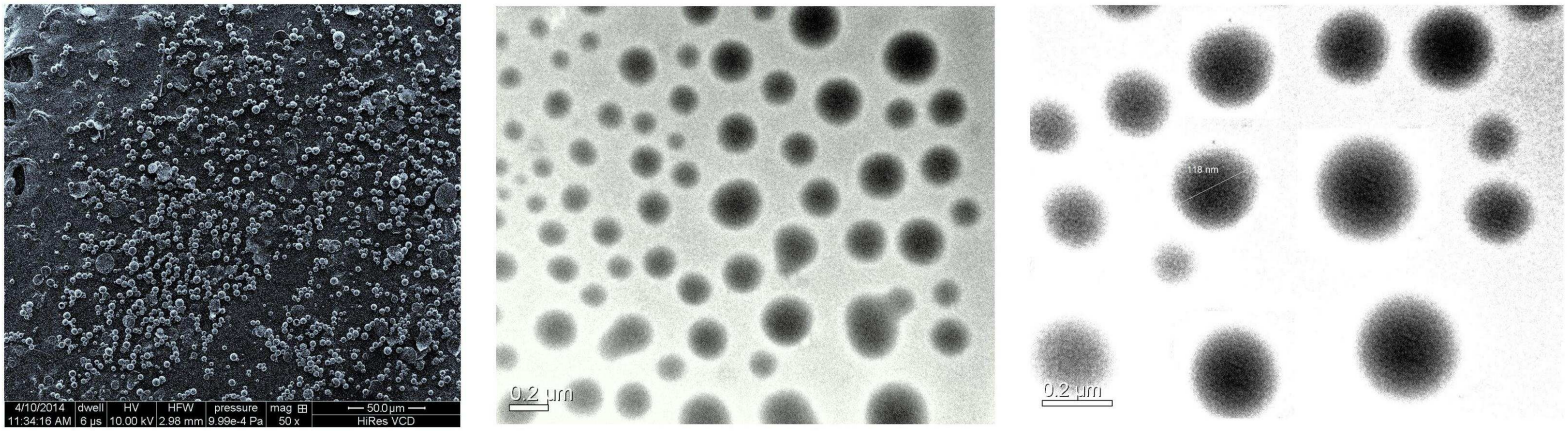

(a) (b) (c)

Fig. 5. (a) Scanning electron microscopy image of prepared micelles, (b, c) transmission electron microscopy images of micelle dispersed within the formulation CAT-3S.

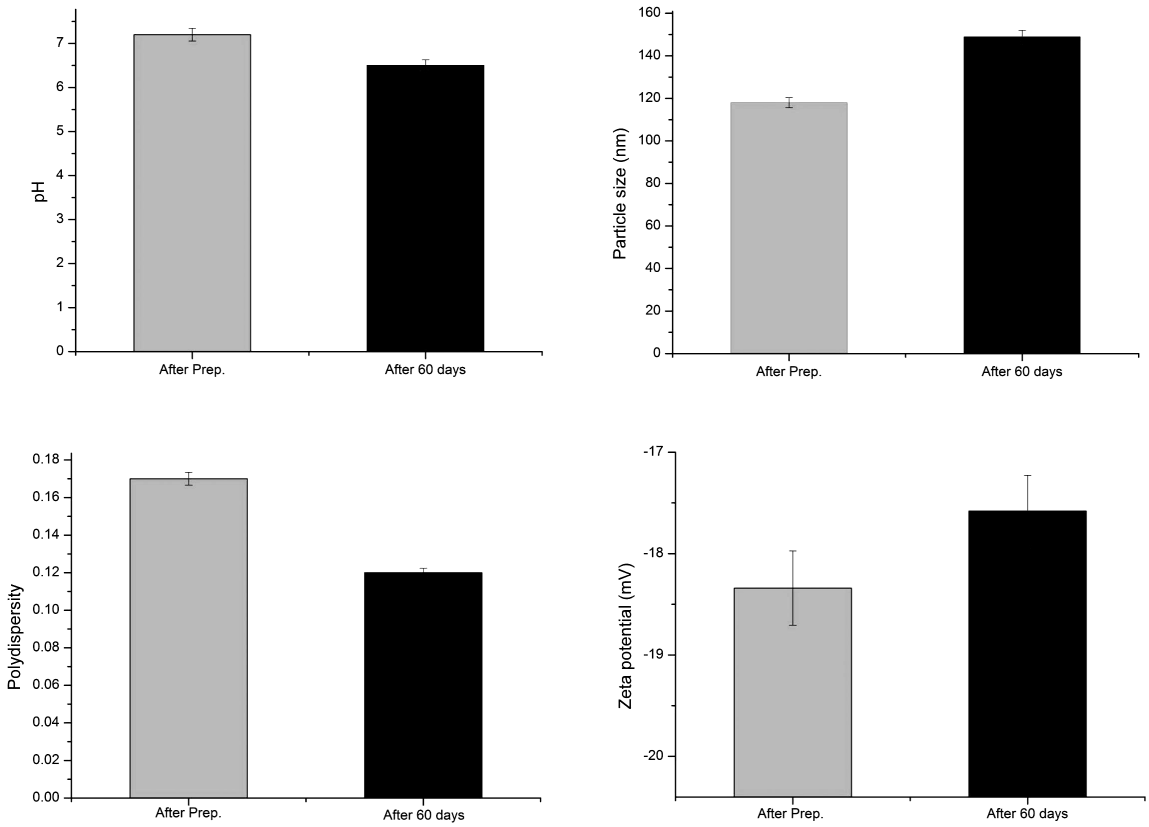

Fig. 6. pH, particle size (nm), polydispersity and zeta potential (mV) of micellar structure, after preparation and after 60 days.

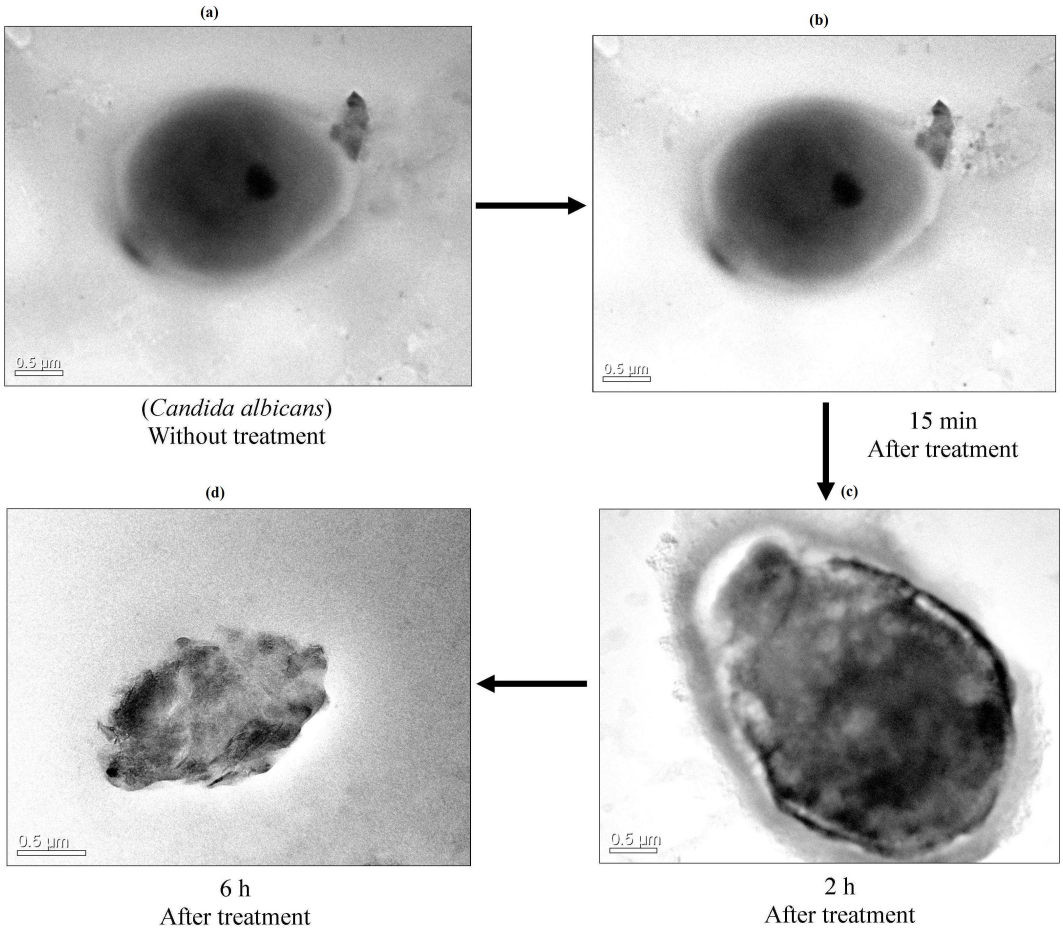

Fig. 7. TEM images of an unexposed (control) cell and CAT-3S (10 µg/ml) treated cell of *C. albicans*.

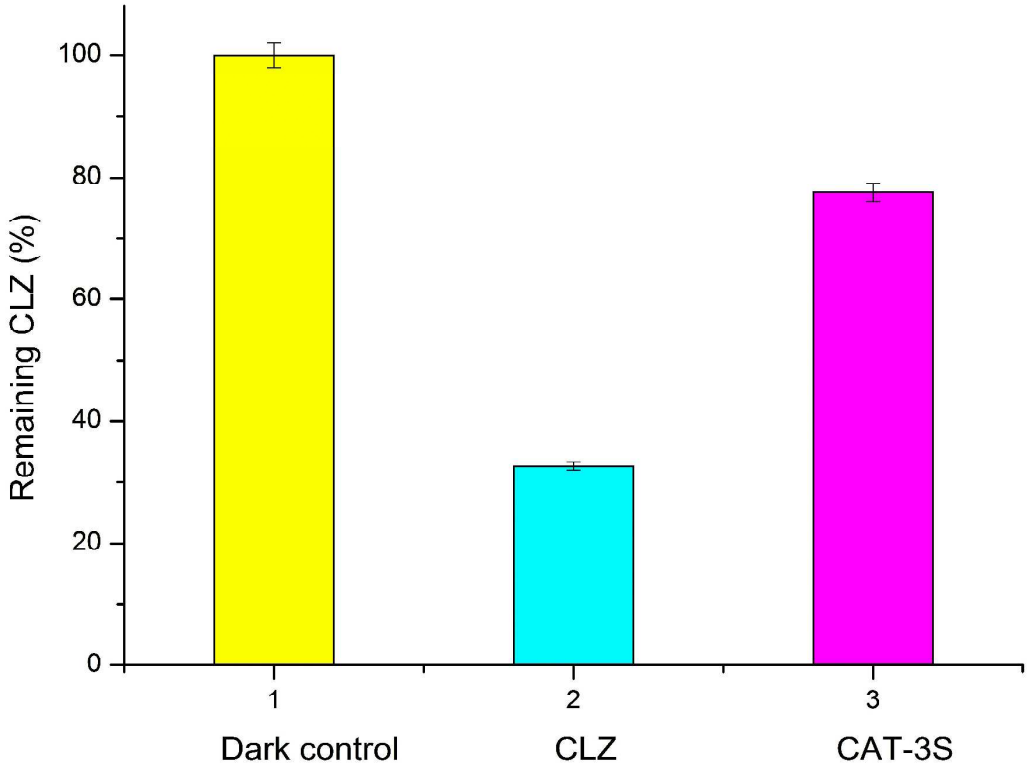

Fig. 8. Plot representing clotrimazole (CLZ) content after 14 h exposure to UV radiations.

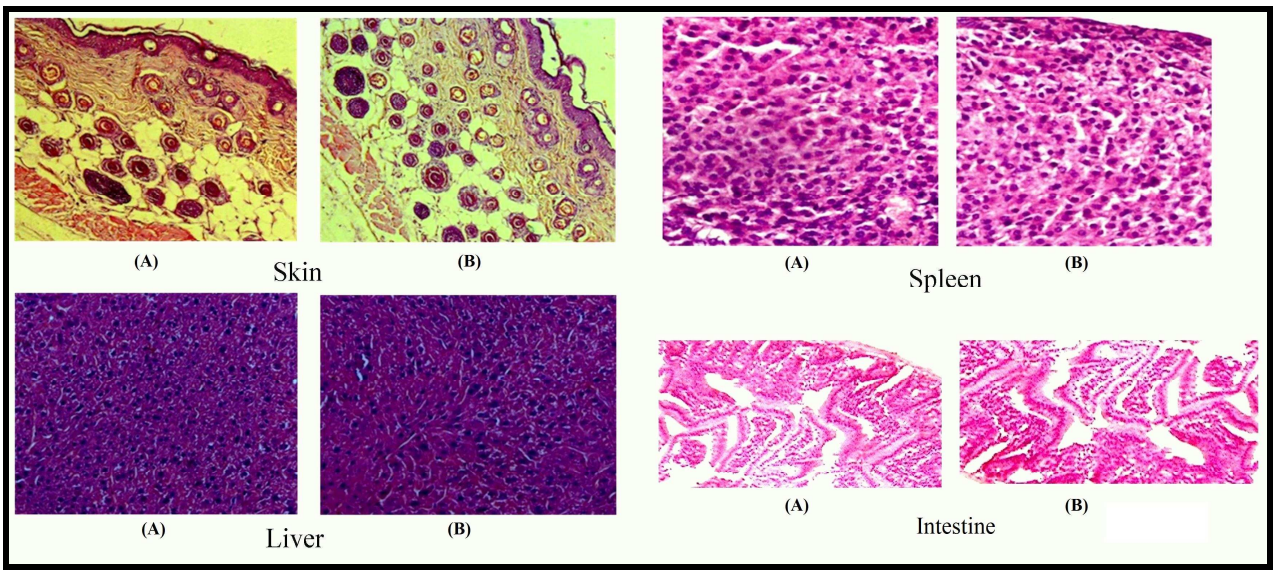

Fig. 9. Histological images of major organs (A) untreated and (B) formulation (CAT-3S) treated, suggesting no toxicity.

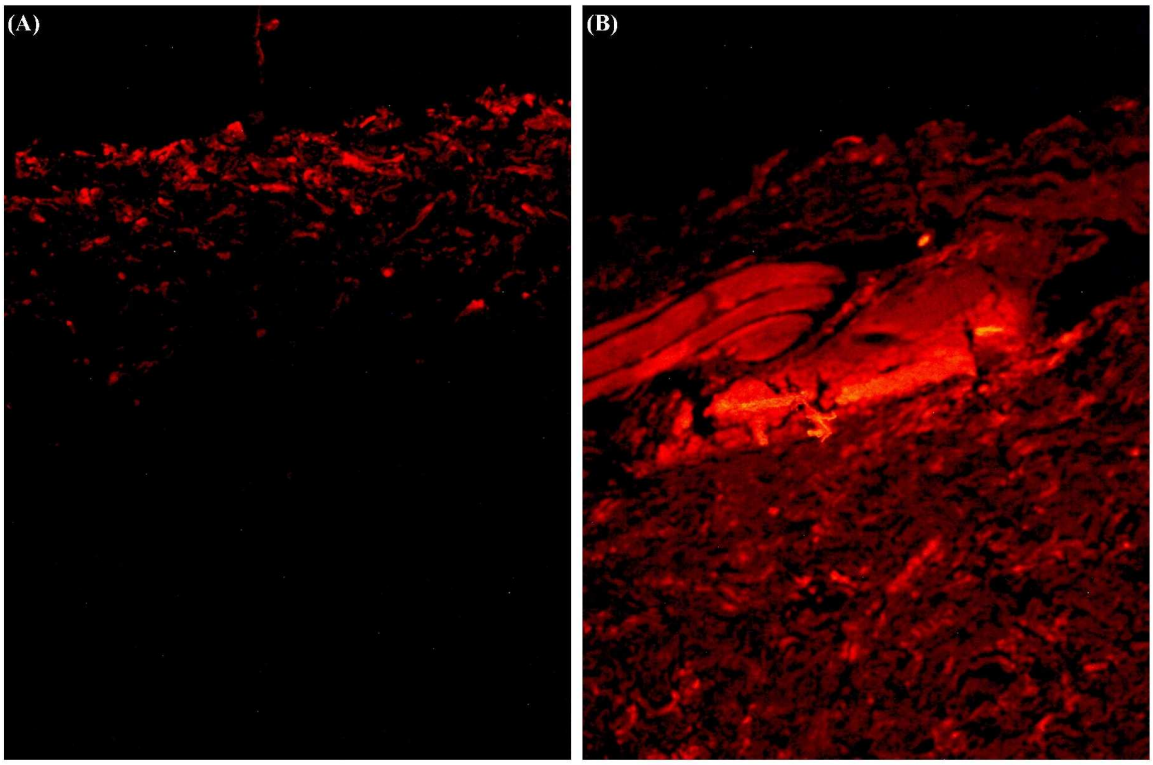

Fig. 10. Confocal laser scanning micrograph of rat skin (A) treatment with hydroalcoholic solution of Rhodamine B, and (B) CAT-3S (Rhodamine B in polymeric system).

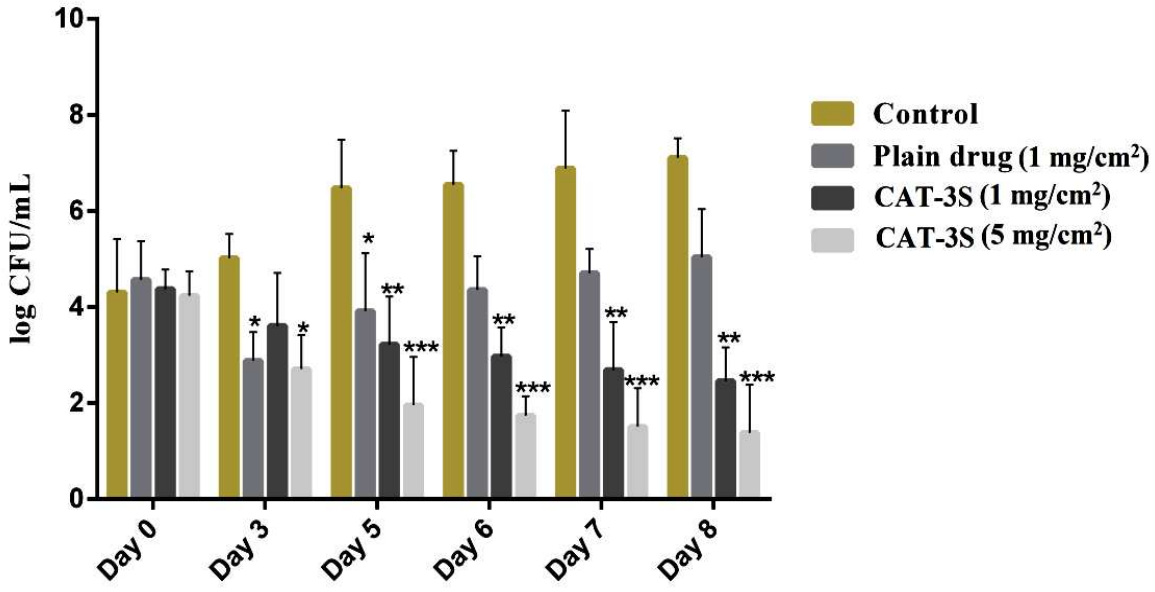

Figure. 11. *In vivo* antifungal activity representing the infection burden in 8 days mouse model.